



New algorithms for blind recognition of OFDM based systems

Abdelaziz Bouzegzi^a, Philippe Ciblat^b, Pierre Jallon^{a,*}

^a CEA-LETI, MINATEC, Grenoble, France

^b ENST, Paris, France

ARTICLE INFO

Article history:

Received 5 May 2009

Received in revised form

1 September 2009

Accepted 17 September 2009

Available online 23 September 2009

Keywords:

Cognitive radio

Blind system recognition

OFDM

Cyclostationarity

Maximum likelihood

Kurtosis

ABSTRACT

In the context of cognitive radio or military applications, it is a crucial task to distinguish blindly various OFDM based systems (e.g., Wifi, Wimax, 3GPP/LTE, DVB-T) from each others. Existing OFDM based systems differ from their subcarrier spacing used in OFDM modulation. One can thus carry out recognition algorithms based on the value of the subcarrier spacing. Standard approaches developed in the literature rely on the detection of the cyclic prefix which enables to exhibit the value of the used subcarrier spacing. Nevertheless these approaches fail when either the cyclic prefix duration is small or the channel impulse response is almost as large as the cyclic prefix. Therefore we propose four new algorithms to estimate the parameters of OFDM modulated signal (especially the subcarrier spacing) relying on (i) the normalized kurtosis, (ii) the maximum-likelihood principle, (iii) the matched filter, and (iv) the second-order cyclostationary property. We show the strong robustness of proposed algorithms to short cyclic prefix, multipath channel, time offset, and frequency offset. Comparisons between proposed algorithms and the state of art techniques are done by means of computer simulations.

© 2009 Elsevier B.V. All rights reserved.

1. Introduction

The blind characterization of digital communication systems has been widely studied in the past decade for military applications. These studies have given rise to many contributions dealing with the identification of the parameters of single carrier signals modulated by linear modulations [1] or by CPM [2]. Concerning OFDM signals identification, only a few papers can be found in the literature [3–10]. This small amount of papers can be explained by the fact that OFDM based systems have emerged only for a few years. The introduction of the cognitive radio concept by [11], which relies on developing flexible terminals able to adapt their transmission parameters to their spectral environment, needs the

receiver to sense its electro-magnetic environment and to identify the surrounding operating systems. Indeed, if opportunistic spectrum access is allowed in some bands of frequencies, an opportunistic receiver working has to be able to distinguish the different kind of base station in these bands, i.e., able to distinguish different modulations. In this context, the carrier frequency f_0 is hence not relevant to characterize the system.

As OFDM modulations are now used in most of popular standards, the receiver should recognize systems based on OFDM modulations. As most of the popular OFDM based standards use different subcarrier spacing (e.g., 15.625, 10.94, 312.5, 1.116, 15 kHz for fixed WiMAX, Mobile WiMAX, WiFi, DVBT, 3GPP/LTE respectively), it is sufficient to estimate the subcarrier spacing of an OFDM modulated signal to identify the encountered systems. Moreover in order to distinguish different modes of a same standard or military context, it should also be useful to estimate the cyclic prefix length. Furthermore, for military applications, a time and frequency

* Corresponding author.

E-mail addresses: abdelaziz.bouzegzi@cea.fr (A. Bouzegzi), philippe.ciblat@enst.fr (P. Ciblat), pierre.jallon@cea.fr (P. Jallon).

synchronization step is crucial since the final objective is information retrieval. As the main objective for cognitive radio applications is only system identification, the time and frequency synchronization step may be optional.

In this paragraph, we remind the main results available in the literature about the subcarrier spacing blind estimation. In the case of cyclic prefixed (CP) OFDM, i.e., the most conventional OFDM, the existing papers propose to extract the OFDM parameters (useful symbol part duration which is equal to the inverse of the subcarrier spacing; cyclic prefix duration) from the correlation induced by the cyclic prefix. For instance, [9] first suggested to estimate the useful part duration by searching the peak of the autocorrelation function which may occur at a time lag equal to the useful part duration. Once the useful part duration is correctly estimated, the estimation of the whole symbol duration¹ is performed using the smallest non-null cyclic frequency. In [8], same estimators are proposed for the useful part and cyclic prefix durations. The authors added the frame length estimation which is obtained by using the correlation between the pilot symbols inserted at the beginning of each frame. In [7], a likelihood function between the cyclic prefix samples and the useful part samples for which the cyclic prefix is copied from is derived in the context of additive white Gaussian noise (AWGN) channel. The deduced cost function shows a great similitude with that proposed in [9]. Recently, [6] proposed to estimate the OFDM parameters with a three steps algorithm: they first considered the OFDM modulation as a linear modulation of symbols and estimates the symbol rate thanks to the cyclostationarity test of [12]. Then, the autocorrelation based method introduced in [9] is used to extract the useful part duration. Finally, the length of the cyclic prefix is estimated by means of cyclostationarity test.

The methods inspected in previous papers are all based on the fact that the cyclic prefix is identical to a portion of the useful part at the receiver side if an AWGN channel is considered. Then the induced correlation enables to estimate the OFDM parameters. All these methods suffer from the same drawback: when the power of the autocorrelation of the received signal is weak, the performance of such algorithms is poor. Unfortunately when the ratio between the cyclic prefix duration and the useful part is small (e.g., this ratio can be equal to $\frac{1}{32}$ in WiMAX and DVB systems) or when the length of the channel impulse response is close to the cycle prefix length, the induced autocorrelation is weak and such algorithms fall down. Notice that simulations in the mentioned papers were often done in AWGN context and/or large cyclic prefix preventing to exhibit this phenomenon.

In [10], the particular context of zero-padded (ZP) OFDM is treated. The method exploited the fact that the autocorrelation function is time-periodic with period equal to the whole symbol duration. Consequently, the whole symbol duration can be estimated first by detecting

the smallest non-null cyclic frequency. Secondly, as null samples are inserted between two OFDM symbols, an entropy criterion is used to discriminate between the guard time and the useful part.

In this paper, four new methods are proposed. These four methods providing an estimation of the OFDM parameters (the useful part length and the cyclic prefix length) are robust to the context of small guard time compared to the useful part and of the channel impulse response as long as the guard time. Consequently, whereas the autocorrelation based method fails in these contexts, our four methods still work well. Our four methods are based on the following different principles: (i) kurtosis minimization, (ii) maximum likelihood, (iii) matched filter, and (iv) cyclic frequency estimation.

The paper is organized as follows: in Section 2, we briefly recall the OFDM signal model. In Section 3, three methods also performing time and frequency offset synchronization steps are described: the first one is based on the kurtosis minimization, the second one on the maximum likelihood and the third one on the matched filter principle. In Section 4, a novel method which does not need prior synchronization step is developed; it is based on the cyclic correlation of the received signal. Section 5 is devoted to numerical simulations. We especially inspect the robustness of our four algorithms to the presence of small cyclic prefix, multipath channel and synchronization errors. Comparison with autocorrelation based method is done. In Section 6, conclusions are drawn.

2. Signal model

The transmitted continuous-time OFDM signal writes

$$s_a(t) = \frac{1}{\sqrt{N}} \sum_{k=0}^{K-1} \sum_{n=0}^{N-1} a_{k,n} e^{-2i\pi n(t-DT_c-kT_s)/NT_c} g_a(t-kT_s), \quad (1)$$

where the sequence $a_{k,n}$ represents the transmit unknown data symbols at subcarrier n and OFDM block k . These data symbols are assumed to be independent and identically distributed (i.i.d). N is the number of subcarriers and $1/T_c$ is the information symbol rate in the absence of guard interval. The inter-carrier spacing is then equal to $1/NT_c$. The length of the cyclic prefix is set to DT_c . The duration of the whole OFDM symbol is then equal to $T_s = (N + D)T_c$. The shaping filter $g_a(t)$ is assumed to be equal to 1 if $0 \leq t < T_s$ and 0 otherwise. A transmission of K OFDM symbols has been considered. For sake of simplicity, we omit to introduce the ZP-OFDM scheme. Nevertheless, as it will be explained latter, the first three proposed algorithms can be also carried out with minor and straightforward modifications in ZP-OFDM context.

The transmitted signal passes through a noisy multipath fading channel composed by L paths. The amplitude and the delay of the l th path are denoted by λ_l and τ_l , respectively. Then the continuous-time received signal takes the following form:

$$y_a(t) = \left(\sum_{l=1}^L \lambda_l s_a(t - \tau_l) \right) e^{2i\pi\delta f t} + b_a(t), \quad (2)$$

¹ Notice the estimated whole symbol duration minus the estimated useful part duration leads to the estimated cyclic prefix duration.

where $b_a(t)$ is a circularly symmetric zero-mean white Gaussian noise with variance σ^2 per complex dimension, and where δf is the frequency offset due to local oscillator drift or Doppler effect.

The continuous-time received signal $y_a(t)$ is sampled at sampling frequency $1/T_e$ where T_e is the sampling period. In order to satisfy the Shannon condition, the sampling frequency must be larger than the OFDM signal bandwidth, i.e., greater than $1/T_c$. Let T_0 be the observation window duration. Let $M = \lfloor T_0/T_e \rfloor$ be the number of available samples where $\lfloor X \rfloor$ stands for the largest integer not greater than X . Then the discrete-time received signal is denoted by $y(m) = y_a(mT_e)$ and writes as

$$y(m) = \left(\sum_{l=1}^L \lambda_l s_a(mT_e - \tau_l) \right) e^{2i\pi\Delta f m} + b(m) \quad (3)$$

with $b(m) = b_a(mT_e)$, and $\Delta f = \delta f T_e$ the normalized carrier frequency offset.

Replacing Eq. (1) into Eq. (3) leads to the following input/output model:

$$y(m) = \frac{1}{\sqrt{N}} \sum_{l=1}^L \sum_{k=0}^{K-1} \sum_{n=0}^{N-1} \lambda_l e^{2i\pi n \tau_l / NT_c} a_{k,n} e^{-2i\pi n m T_e / NT_c} e^{2i\pi (k+1) DT_c / NT_c} \times g_a(mT_e - \tau_l - k(N+D)T_c) e^{2i\pi\Delta f m} + b(m). \quad (4)$$

In practice the cognitive terminal just has the knowledge of $\{y(m)\}_{m=0}^{M-1}$, M , T_0 , T_e and wishes to estimate the values of N , NT_c , DT_c . For selecting the used standard, the cognitive terminal firstly needs the knowledge of the subcarrier spacing given by the inverse of NT_c . Notice that in Eq. (4), K , $a_{k,n}$, L , $\{\lambda_l, \tau_l\}_{l=1}^L$, and Δf are unknown as well.

Methods introduced in Section 3.1 (based on kurtosis optimization) and Section 4 (based on cyclic correlation) rely on signal model provided by Eq. (4). In contrast methods introduced in Section 3.2 (based on maximum likelihood) and Section 3.3 (based on matched filter) assume an AWGN channel, i.e., $L = 1$, $\lambda_1 = 1$, and $\tau_1 = 0$. However, impact and robustness of a multipath channel on these methods are addressed in Section 5 devoted to numerical computations.

3. OFDM parameters estimation with synchronization step

In this section, we present three novel methods to perform the estimation of the OFDM parameters. These methods either need a prior step of time and frequency synchronization or insert a synchronization step into their computations. Albeit high computational load, especially due to the extra synchronization step, our proposed methods are worth since they outperform the existing autocorrelation based method as shown in Section 5. In this section, only CP-OFDM is considered. However, extension to other kind of OFDM (like ZP-OFDM) is straightforward, and is omitted hereafter due to the lack of space.

This long section is actually organized as follows. Section 3.1 is devoted to the kurtosis optimization based method. Section 3.2 focuses on the maximum likelihood

based method. Finally, the matched filter based method is introduced in Section 3.3. In this section, notice that, except otherwise stated, the prior synchronization is assumed to be carried out. Algorithm adaptation to time and frequency missynchronization scheme is done at the end of each subsection. Moreover, empirical performance in the realistic context of time and frequency missynchronization is assessed in Section 5.

3.1. Kurtosis minimization based method

3.1.1. Algorithm description

The first new algorithm needs an adaptive receiver which depends on the three following parameters \tilde{N} , \tilde{NT}_c , and \tilde{DT}_c where \tilde{N} , \tilde{NT}_c , and \tilde{DT}_c are trial values for N , NT_c , and DT_c , respectively. To simplify the presentation, we first assume (i) that the received signal is noiseless, and (ii) that the first received samples $y(0)$ matches the beginning of an OFDM symbol (perfect time synchronization) and $\Delta f = 0$ (perfect frequency synchronization).

The adaptive receiver works as follows:

1. Split the received samples into estimated OFDM symbols:

$$r_{k,p} = y_a(pT_e + \tilde{DT}_c + k(\tilde{NT}_c + \tilde{DT}_c)). \quad (5)$$

In the sequel, we substitute \tilde{P} with $\lfloor \tilde{NT}_c/T_e \rfloor$ and \tilde{K} is the estimate of the number of OFDM symbols within the observation time. Note that if $\tilde{NT}_c = NT_c$ and $\tilde{DT}_c = DT_c$, then $r_{k,p}$ corresponds to the p th element of the k th OFDM block once the cyclic prefix has been removed.

2. Estimate the transmit data symbols by applying the normalized Fourier transform as follows:

$$\forall n \in \{0, \dots, \tilde{N} - 1\}, \quad \hat{a}_{k,n} = \frac{1}{\sqrt{\tilde{P}}} \sum_{p=0}^{\tilde{P}-1} r_{k,p} e^{2i\pi p n T_e / \tilde{NT}_c}. \quad (6)$$

The first new algorithm is based on the following idea: if the trial values \tilde{NT}_c and \tilde{DT}_c match with the true values of NT_c and DT_c , respectively, then the decoded symbol $\hat{a}_{k,n}$ at block k and at subcarrier n is expected to depend only on one of the transmitted symbols (for example $a_{k,n}$). The idea can be mathematically translated as follows: it exists an unknown constant μ_n depending only on the channel frequency response such that

$$\hat{a}_{k,n} = \mu_n a_{k,n}. \quad (7)$$

On the contrary, if the OFDM parameters are misestimated, i.e., $\tilde{NT}_c \neq NT_c$ and/or $\tilde{DT}_c \neq DT_c$, then an extra term associated with inter-carrier and/or inter-symbol interference should appear in Eq. (7).

In order to ensure that our estimation algorithm forces the adaptive receiver to satisfy Eq. (7), we need a criterion for which the optimization on \tilde{NT}_c and \tilde{DT}_c prevents interference at the receiver side. Therefore, as done in blind channel deconvolution [13,14] we advocate to use

the kurtosis of the estimated symbols which is defined as

$$\kappa(\hat{a}_{k,n}) = \frac{\text{cum}(\hat{a}_{k,n}, \hat{a}_{k,n}^*, \hat{a}_{k,n}, \hat{a}_{k,n}^*)}{(\mathbb{E}[|\hat{a}_{k,n}|^2])^2}, \quad (8)$$

where the superscript $(\cdot)^*$ stands for the complex conjugate.

Our objective is hence to prove that the kurtosis of each decoded symbol defined as a function of \widetilde{NT}_c and \widetilde{DT}_c reaches its global minimum value if and only if $\widetilde{NT}_c = NT_c$ and $\widetilde{DT}_c = DT_c$. Once this theoretical result is proved,

$$\hat{\kappa}(\hat{a}_{k,v}) = \frac{\sum_{k=0}^{\widetilde{M}-1} \sum_{v=0}^{\widetilde{N}-1} |\hat{a}_{k,v}|^4 - |\sum_{k=0}^{\widetilde{M}-1} \sum_{v=0}^{\widetilde{N}-1} (\hat{a}_{k,v})^2|^2 - 2(\sum_{k=0}^{\widetilde{M}-1} \sum_{v=0}^{\widetilde{N}-1} |\hat{a}_{k,v}|^2)^2}{(\sum_{k=0}^{\widetilde{M}-1} \sum_{v=0}^{\widetilde{N}-1} |\hat{a}_{k,v}|^2)^2} \quad (9)$$

we will be in position to develop a practical estimation algorithm of NT_c and DT_c based on the minimization of the kurtosis.

Before going further, in order to simplify forthcoming derivations, we remark that the transmit symbols $a_{k,n}$ are i.i.d. symbols; their kurtosis $\kappa(a_{k,v})$ thus do not depend on k nor v , and it will be denoted by $\kappa(a)$. We remind that the kurtosis is negative for standard linear modulations (PAM, PSK, QAM) [3].

Now we introduce the main results of this subsection related to the proof of the convergence of the kurtosis optimization to the true values of the OFDM parameters.

Theorem 1. Consider the decoded symbols at subcarrier v and OFDM symbol k . We have the following result:

Given (k, v) , $\kappa(\hat{a}_{k,v}) \geq \kappa(a)$

and the equality is achieved if and only if

- $\forall p \in \{0, \widetilde{P} - 1\}$, the samples $r_{k,p}$ from which are extracted $\hat{a}_{k,v}$ (see Eq. (5)) belong to the same transmitted OFDM symbol, and
- $\widetilde{NT}_c = NT_c$.

If the equality holds, we also have $\hat{a}_{k,v} = \mu_v a_{k,v}$ with μ_v a constant depending on subcarrier v .

In fact, one can prove the previous inequality for any subcarrier v and any OFDM symbol k , i.e., we have

$$\forall (k, v), \quad \kappa(\hat{a}_{k,v}) \geq \kappa(a)$$

and the equality is achieved if and only if

- $\widetilde{NT}_c = NT_c$, and
- $\widetilde{DT}_c = DT_c$.

Proof of Theorem 1 is given in Appendix A.

We remark that $\hat{a}_{k,v}$ corresponds to the symbol transmitted at the carrier v , but not necessarily at the k th OFDM symbol. Moreover the proposed algorithm has a very low sensitivity to \widetilde{N} . The algorithm works well if this parameter is under-estimated. Consequently it can be chosen equal to 64 since most of OFDM systems use at least 64 subcarriers. To estimate accurately N , once NT_c

and DT_c have been estimated, several standard techniques can be employed such that the Gaussianity test on each subcarrier. Estimation of N is out of the scope of the paper since the value of N does not allow to distinguish systems from each other.

The question now is: How to estimate the kurtosis of the decoded sequence of symbols $\hat{a}_{k,n}$? For instance, we get $\text{cum}(\hat{a}_{k,n}, \hat{a}_{k,n}^*, \hat{a}_{k,n}, \hat{a}_{k,n}^*) = \mathbb{E}[|\hat{a}_{k,v}|^4] - |\mathbb{E}[\hat{a}_{k,v}^2]|^2 - 2(\mathbb{E}[|\hat{a}_{k,v}|^2])^2$. Then, when trial values $\widetilde{N}(=64)$, \widetilde{NT}_c , and \widetilde{DT}_c are used, $\kappa(\hat{a}_{k,v})$ can be usually estimated by $\hat{\kappa}(\hat{a}_{k,v})$ defined as follows:

with $\widetilde{M} = \lfloor M/(\widetilde{NT}_c + \widetilde{DT}_c) \rfloor$.

Actually $\hat{\kappa}(\hat{a}_{k,v})$ is a function of \widetilde{NT}_c and \widetilde{DT}_c and will be the cost function of our first new algorithm associated with kurtosis minimization (KM). Now denoting $\hat{\kappa}(\hat{a}_{k,v})$ by $\hat{J}_{\text{KM}}(\widetilde{NT}_c, \widetilde{DT}_c)$, we have

$$[\widetilde{NT}_c, \widetilde{DT}_c] = \arg \min_{\widetilde{NT}_c, \widetilde{DT}_c} \hat{J}_{\text{KM}}(\widetilde{NT}_c, \widetilde{DT}_c). \quad (10)$$

Theorem 1 ensures that the minimization procedure given in Eq. (10) leads to the identifiability of NT_c and DT_c in noiseless context and infinite number of available samples. In practice (i.e., when the signal is noisy and when only a finite number of observations are available), we can only conjecture that \widetilde{NT}_c and \widetilde{DT}_c are close to NT_c and DT_c , respectively, if the noise is not so strong and if the number of available samples is large enough.

3.1.2. Adaptation to time and frequency missynchronization

We consider that $\min_l \tau_l = \tau_{\min} > 0$. Due to this time offset, the blind OFDM receiver should ensure that its first sample $r_{0,0}$ depends on the transmitted signal. For doing that, a preliminary step has to be added to the receiver. This step consists in dropping the first $\tilde{\tau}$ samples where $\tilde{\tau}$ is a trial value for τ_{\min} .

Similarly, if the received signal undergoes a carrier frequency offset ($\Delta f \neq 0$), another extra step has to be added to the receiver to estimate and compensate it. The received samples given by Eq. (5) should then be modified into

$$r_{k,p} = y_a(pT_e + \widetilde{DT}_c + k(\widetilde{NT}_c + \widetilde{DT}_c))e^{-2i\pi\Delta f(pT_e + \widetilde{DT}_c + k(\widetilde{NT}_c + \widetilde{DT}_c))/T_e}, \quad (11)$$

where $\widetilde{\Delta f}$ is a trial value of Δf .

The cost function has to be modified accordingly by adding two parameters. Then we have

$$[\tau_{\min}, \widetilde{\Delta f}, \widetilde{NT}_c, \widetilde{DT}_c] = \arg \min_{\tau_{\min}, \widetilde{\Delta f}, \widetilde{NT}_c, \widetilde{DT}_c} \hat{J}_{\text{KM}}(\tilde{\tau}, \widetilde{\Delta f}, \widetilde{NT}_c, \widetilde{DT}_c)$$

with

$$\hat{J}_{\text{KM}}(\tilde{\tau}, \widetilde{\Delta f}, \widetilde{NT}_c, \widetilde{DT}_c) = \frac{\sum_{k=0}^{\widetilde{M}-1} \sum_{v=0}^{\widetilde{N}-1} |\hat{a}_{k,v}|^4 - |\sum_{k=0}^{\widetilde{M}-1} \sum_{v=0}^{\widetilde{N}-1} (\hat{a}_{k,v})^2|^2 - 2(\sum_{k=0}^{\widetilde{M}-1} \sum_{v=0}^{\widetilde{N}-1} |\hat{a}_{k,v}|^2)^2}{(\sum_{k=0}^{\widetilde{M}-1} \sum_{v=0}^{\widetilde{N}-1} |\hat{a}_{k,v}|^2)^2}$$

With similar techniques developed in Appendix A, one can prove that Theorem 1 still holds and induces also the equalities $\tau_{\min} = \tau_{\min}$ and $\hat{\Delta}f = \Delta f$.

3.2. Maximum likelihood based method

This subsection is organized as follows: in Section 3.2.1, we describe the received signal thanks to matrix framework. In Section 3.2.2, we focus on the so-called *deterministic* maximum likelihood. The so-called *Gaussian* maximum likelihood is introduced in Section 3.2.3.

These algorithms require prior synchronization step or can be adapted similarly to Section 3.1.2 associated with kurtosis minimization algorithm by adding once again a synchronization step into the next proposed cost functions.

In order to get tractable closed-form expressions, an AWGN channel model is considered in this subsection. Robustness to multipath channel is evaluated in Section 5.

3.2.1. Matrix framework

We assume AWGN channel and perfect time and frequency synchronization.

Let

- $\mathbf{a}_k = [a_{k,0}, \dots, a_{k,N-1}]^T$
- $\mathbf{a} = [\mathbf{a}_0^T, \dots, \mathbf{a}_{K-1}^T]^T$
- $\mathbf{b} = [b(0), \dots, b(M-1)]^T$

where the superscript $(\cdot)^T$ stands for the transpose operator.

We stack all the received samples in the following vector $\mathbf{y} = [y(0), \dots, y(M-1)]^T$. Using Eq. (4) under AWGN and perfect synchronization assumptions ($L = 1$, $\lambda_1 = 1$, $\tau_1 = 0$, and $\Delta f = 0$), we have

$$\mathbf{y} = \mathbf{F}_\theta \mathbf{a} + \mathbf{b}, \quad (12)$$

where $\theta = [N, NT_c, DT_c]$ denotes the set of OFDM parameters and \mathbf{F}_θ is a matrix expressed as below. As $g_a(t)$ is a rectangular function, Eq. (4) leads to the following constraint:

$$0 \leq mT_e - k(N+D)T_c < (N+D)T_c,$$

which implies that

$$m \frac{T_e}{(N+D)T_c} - 1 < k \leq m \frac{T_e}{(N+D)T_c}.$$

Consequently, for a given m , it exists only a unique value of k , denoted by k_m . \mathbf{F}_θ is then composed of null components except the next ones

$$[\mathbf{F}_\theta]_{m, k_m N + n} = \frac{1}{\sqrt{N}} e^{2i\pi n m T_e / NT_c} e^{2i\pi n (k_m + 1) DT_c / NT_c} \quad (13)$$

for $m = 0, \dots, M-1$ and $n = 0, \dots, N-1$. Term $[\mathbf{F}_\theta]_{m, k_m N + n}$ corresponds to the element of the m th row and $(k_m N + n)$ th column of \mathbf{F}_θ .

As the transmit data \mathbf{a} are unknown at the receiver, the likelihood of \mathbf{y} given N, DT_c, NT_c , and \mathbf{a} has to be averaged over \mathbf{a} . The true maximum-likelihood based estimator of N, DT_c , and NT_c is then complex to be carry out. To overcome the problem, we propose either to consider

vector \mathbf{a} as parameters of interest too which leads to the so-called deterministic maximum likelihood or to consider vector \mathbf{a} as Gaussian (even if \mathbf{a} is not Gaussian vector) which leads to the so-called Gaussian maximum-likelihood [15].

3.2.2. Deterministic maximum-Likelihood approach (DML)

Let $p(\mathbf{y}|\theta, \mathbf{a})$ be the likelihood of \mathbf{y} given θ and \mathbf{a} . The deterministic maximum-likelihood is defined as follows [15]:

$$[\hat{N}, \hat{DT}_c, \hat{NT}_c, \hat{\mathbf{a}}] = \underset{\theta, \mathbf{a}}{\operatorname{argmax}} p(\mathbf{y}|\theta, \hat{\mathbf{a}}).$$

As we assume the transmitted symbols \mathbf{a} deterministic, and thanks to (12), the vector $\hat{\mathbf{a}}$ writes $(\mathbf{F}_\theta^H \mathbf{F}_\theta)^{-1} \mathbf{F}_\theta^H \mathbf{y}$.

In practice, the signal bandwidth (given by $1/T_c$) can be assumed to be roughly known. This enables us to choose a reasonable value for $1/T_e$ and also to filter the received signal by an ideal low-pass filter of unit-magnitude and bandwidth $1/T_c$. This induces that the discrete-time noise has the following autocorrelation function:

$$r_b(n) = \mathbb{E}[b(m+n)\overline{b(m)}] = \frac{2N_0}{T_c} \operatorname{sinc}\left(\frac{\pi n}{q}\right)$$

with $q = T_c/T_e$ the sampling factor. The discrete-time noise is not white. In order to simplify the DML estimator, the discrete-time noise will be, however, assumed to be white. Obviously, in the simulation part, the noise process color will not be neglected.

By assuming the noise vector \mathbf{b} uncorrelated and by considering $KN \leq M$, it is well known that the DML estimator can take the following form [15]:

$$[\hat{N}, \hat{NT}_c, \hat{DT}_c] = \underset{N, NT_c, DT_c}{\operatorname{arg\,min}} \hat{J}_{\text{DML}}(\hat{N}, \hat{NT}_c, \hat{DT}_c) \quad (14)$$

with

$$\hat{J}_{\text{DML}}(\hat{N}, \hat{NT}_c, \hat{DT}_c) = \|\mathbf{I} - \mathbf{F}_\theta (\mathbf{F}_\theta^H \mathbf{F}_\theta)^{-1} \mathbf{F}_\theta^H \mathbf{y}\|, \quad (15)$$

$\tilde{\theta} = [\hat{N}, \hat{NT}_c, \hat{DT}_c]$ and where $(\cdot)^H$ stands for the conjugate-transposition.

3.2.3. Gaussian maximum-likelihood approach (GML)

In this subsection, the transmit data vector \mathbf{a} is assumed to be an i.i.d. random vector. Its true power density function (pdf) is a product of a sum of Dirac distribution for which the location is given by the used constellation (either PAM or PSK or QAM). Due to the high complexity of derivations, it is usual to model the vector \mathbf{a} as a circularly symmetric Gaussian multivariate process with zero mean and covariance σ_a^2 per real dimension [15]. Then the so-called Gaussian likelihood, denoted by $p_g(\mathbf{y}|\theta)$, can be expressed in closed-form when \mathbf{a} is assumed as above.

Consequently the multivariate process \mathbf{y} is circularly symmetric Gaussian process with zero mean and covariance matrix $\mathbb{E}[\mathbf{y}\mathbf{y}^H] = 2\sigma_a^2 \mathbf{F}_\theta \mathbf{F}_\theta^H + 2N_0 \mathbf{I}_M$ and yields the

following likelihood:

$$p_g(\mathbf{y}|\theta) = \frac{1}{(2\pi)^M \det(2\sigma_a^2 \mathbf{F}_\theta \mathbf{F}_\theta^H + 2N_0 \mathbf{I}_{d_M})} e^{-\frac{1}{2} \mathbf{y}^H (\sigma_a^2 \mathbf{F}_\theta \mathbf{F}_\theta^H + N_0 \mathbf{I}_{d_M})^{-1} \mathbf{y}}.$$

Let \mathbf{I}_d and \mathbf{A} be the identity matrix and another matrix compatible in size, respectively. We remind that $\det(\mathbf{I}_d + \mathbf{A}\mathbf{A}^H) = \det(\mathbf{I}_d + \mathbf{A}^H\mathbf{A})$ and $(\mathbf{I}_d + \mathbf{A}\mathbf{A}^H)^{-1} = \mathbf{I}_d - \mathbf{A}(\mathbf{I}_d + \mathbf{A}^H\mathbf{A})^{-1} \mathbf{A}^H$. This leads to

$$p_g(\mathbf{y}|\theta) \propto \frac{1}{\det(2\sigma_a^2 \mathbf{F}_\theta^H \mathbf{F}_\theta + 2N_0 \mathbf{I}_{KN})} e^{(\sigma_a^2/N_0) \mathbf{y}^H \mathbf{F}_\theta (2\sigma_a^2 \mathbf{F}_\theta^H \mathbf{F}_\theta + 2N_0 \mathbf{I}_{KN})^{-1} \mathbf{F}_\theta^H \mathbf{y}}.$$

As maximizing $p_g(\mathbf{y}|\theta)$ is equivalent to minimizing $-\log p_g(\mathbf{y}|\theta)$, we get

$$[\hat{N}, \hat{DT}_c, \hat{NT}_c] = \arg \min_{N, NT_c, DT_c} \hat{J}_{\text{GML}}(\tilde{N}, \tilde{NT}_c, \tilde{DT}_c) \quad (16)$$

with

$$\begin{aligned} \hat{J}_{\text{GML}}(\tilde{N}, \tilde{NT}_c, \tilde{DT}_c) &= \log(\det(2\sigma_a^2 \mathbf{F}_{\tilde{\theta}}^H \mathbf{F}_{\tilde{\theta}} + 2N_0 \mathbf{I}_{KN})) \\ &\quad - \frac{\sigma_a^2}{2N_0} \mathbf{y}^H \mathbf{F}_{\tilde{\theta}} (\sigma_a^2 \mathbf{F}_{\tilde{\theta}}^H \mathbf{F}_{\tilde{\theta}} + N_0 \mathbf{I}_{KN})^{-1} \mathbf{F}_{\tilde{\theta}}^H \mathbf{y}. \end{aligned} \quad (17)$$

Notice that \tilde{K} , the trial value for the number of OFDM symbols, depends on the trial value $\tilde{\theta}$ since $\tilde{K} = \lfloor T_0 / (\tilde{DT}_c + \tilde{NT}_c) \rfloor$. Moreover signal-to-noise ratio (provided by σ_a^2/N_0) has to be estimated prior to computing GML estimators. Similar estimator has been already introduced by [16] in the context of symbol period estimation for single carrier modulated signal.

3.3. Matched filter based method

The third new algorithm based on the matched filter (MF) principle is proposed. The time and frequency offsets are handled as for the maximum likelihood based algorithms and the kurtosis minimization based algorithm. Once again, we assume hereafter perfect time and frequency synchronization. This method is introduced in an AWGN context. Numerical analysis of its robustness to multipath channel is done in Section 5.

By inspecting Eq. (4) under AWGN and perfect synchronization assumptions, we see that the matched filter receiver associated with true parameters θ consists in multiplying the receiver signal \mathbf{y} by \mathbf{F}_θ^H following by a decision threshold. One can guess that applying an imperfect matched filter $\mathbf{F}_{\tilde{\theta}}^H$ associated with the trial parameters $\tilde{\theta}$ leads to a degradation of SNR. Therefore we propose to build a criterion related to the maximization of the energy of $\mathbf{F}_{\tilde{\theta}}^H \mathbf{y}$ with respect to $\tilde{\theta}$. As the norm of $\mathbf{F}_{\tilde{\theta}}^H \mathbf{y}$ depends on $\tilde{\theta}$, we finally advocate the use of the following “normalized” cost function

$$[\hat{N}, \hat{DT}_c, \hat{NT}_c] = \arg \max_{N, NT_c, DT_c} J_{\text{MF}}(\tilde{N}, \tilde{NT}_c, \tilde{DT}_c) \quad (18)$$

with

$$J_{\text{MF}}(\tilde{N}, \tilde{NT}_c, \tilde{DT}_c) = \frac{\mathbb{E}[\|\mathbf{F}_{\tilde{\theta}}^H \mathbf{y}\|^2]}{\|\mathbf{F}_{\tilde{\theta}}^H \mathbf{F}_{\tilde{\theta}}\|_F}, \quad (19)$$

where $\|\mathbf{x}\|$ is the Euclidian norm of the vector \mathbf{x} and $\|\mathbf{A}\|_F$ is the Frobenius norm of the matrix \mathbf{A} equal to $\sqrt{\text{Tr}(\mathbf{A}^H \mathbf{A})}$.

In the next theorem, we prove that, in noiseless case, the maximization of cost function $J_{\text{MF}}(\cdot)$ yields the true parameter vector θ which justifies our intuition and the proposed cost function.

Theorem 2. *In noiseless context, we get the following inequality:*

$$\forall \tilde{N}, \tilde{NT}_c, \text{ and } \tilde{DT}_c, \quad J_{\text{MF}}(\tilde{N}, \tilde{NT}_c, \tilde{DT}_c) \leq J_{\text{MF}}(N, NT_c, DT_c).$$

The equality is reached if and only if $[\tilde{N}, \tilde{NT}_c, \tilde{DT}_c] = [N, NT_c, DT_c]$, and then the cost function has the following value $\|\mathbf{F}_\theta \mathbf{F}_\theta^H\|_F$.

Proof of Theorem 2 is given in Appendix B.

The matched filter estimator takes then the following form:

$$[\hat{N}, \hat{DT}_c, \hat{NT}_c] = \arg \max_{N, NT_c, DT_c} \hat{J}_{\text{MF}}(\tilde{N}, \tilde{NT}_c, \tilde{DT}_c),$$

where \hat{J}_{MF} is simply estimated as

$$\hat{J}_{\text{MF}}(\tilde{N}, \tilde{NT}_c, \tilde{DT}_c) = \frac{\|\mathbf{F}_{\tilde{\theta}}^H \mathbf{y}\|^2}{\|\mathbf{F}_{\tilde{\theta}}^H \mathbf{F}_{\tilde{\theta}}\|_F}.$$

4. OFDM parameters estimation without synchronization step

This section is devoted to the presentation and the analysis of the fourth new algorithm. The cyclic prefix in CP-OFDM induces cyclostationarity that can be used to identify the OFDM parameters. This new algorithm relies on this property and is a non-trivial extension of the well-spread autocorrelation based algorithm described in [6–10]. Notice that the algorithm does not require time and frequency synchronization so that we can assume perfect time and frequency synchronization without loss of generality. Moreover, as the multipath channel partially destroys the interesting correlation property induced by the cyclic prefix, the description of the algorithm is done under the assumption of AWGN channel. Nevertheless, robustness of this algorithm to multipath context is inspected in Section 5. We observe that the new algorithm outperforms the autocorrelation based method in realistic context (small cyclic prefix and/or strong multipath channel).

4.1. Cyclic correlation (CC) based method

Let $R_y(n, m) = \mathbb{E}[y(n+m)y^*(n)]$ be the correlation function of the received signal given by Eq. (4) and let us assume to simplify that NT_c/T_e is an integer. In the context of AWGN ($L=1$, $\lambda_1=1$, $\tau_1=0$), the presence of the cyclic prefix induces a correlation since $R_y(n, m)$ does not vanish for the following three values $m =$

0, $\lfloor NT_c/T_e \rfloor, -\lfloor NT_c/T_e \rfloor$. We can hence express the correlation function as follows:

$$R_y(n, m) = R_y(n, 0)\delta(m) + R_y(n, \alpha)\delta(m - \alpha) + R_y(n, -\alpha)\delta(m + \alpha) \quad (20)$$

with $\alpha = \lfloor NT_c/T_e \rfloor$.

In Eq. (20), one can remark that

- The first term of the RHS $R_y(n, 0)$ is equal to $1 + \sigma^2$ and does not provide information about OFDM parameters.
- The second and third terms can be written as follows (see Eq. (4)):

$$R_y(n, \alpha) = \sum_{k \in \mathbb{Z}} g(n + \alpha - k\alpha(1 + \beta))g^*(n - k\alpha(1 + \beta)) \quad (21)$$

with $\beta = DT_c/NT_c = D/N$ and $g(n) = g_a(nT_e)$. These terms provide useful information about OFDM parameters such as NT_c and DT_c . Thus they can be taken into account to build an identification criterion.

Before going further, we notice that $\lfloor \alpha(1 + \beta) \rfloor$ is the number of samples encompassed in a whole OFDM symbol, and $\lfloor \alpha\beta \rfloor$ is the number of samples encompassed in the cyclic prefix.

As $n \mapsto R_y(n, \alpha)$ is a pseudo-periodic function (or a periodic function if $\alpha(1 + \beta)$ is an integer), it can be decomposed into the following Fourier series expansion:

$$R_y(n, \alpha) = \sum_{p \in \mathbb{Z}} R_y^{(p/\alpha(1+\beta))}(\alpha) e^{2i\pi np/\alpha(1+\beta)}, \quad (22)$$

where $R_y^{(p/\alpha(1+\beta))}(\alpha)$ is the cyclic correlation coefficient of the signal y at the cyclic frequency $p/\alpha(1 + \beta)$.

The estimation of the OFDM parameters NT_c and DT_c can be performed through parameters α and β . Indeed, if $\tilde{\alpha}$ and $\tilde{\beta}$ are trial values of α and β , the cyclic correlation $R_y^{(p/\tilde{\alpha}(1+\tilde{\beta}))}(\tilde{\alpha})$ vanishes if $\tilde{\alpha} \neq \alpha$. It also vanishes when $\tilde{\beta} \neq \beta$ if there is no p' such as $p/\tilde{\alpha}(1 + \tilde{\beta}) = p'/\alpha(1 + \beta)$. Consequently, an estimation only based on the term $p = 0$ does not allow to estimate β . Notice that the standard autocorrelation method introduced in [6–10] relies on this principle but it is only based on the cyclic correlation at the cyclic frequency 0.

The method we propose is hence a natural extension by using cyclic correlation at several non-null cyclic frequencies. We thus rely our identification scheme on the maximization of the following cost function:

$$(\tilde{\alpha}, \tilde{\beta}) \mapsto J_{CC}^{(N_b)}(\tilde{\alpha}, \tilde{\beta}) = \frac{1}{2N_b + 1} \sum_{p=-N_b}^{N_b} |R_y^{(p/\tilde{\alpha}(1+\tilde{\beta}))}(\tilde{\alpha})|^2, \quad (23)$$

where N_b is the number of cyclic frequencies taken into account to compute the cost function. This function has to be jointly maximized on $\tilde{\alpha}$ and $\tilde{\beta}$. This 2-D research interval leads to a high computational load of the proposed method. In order to mitigate this load, we mention that usually the true β belongs to the following small set $\{\frac{1}{4}, \frac{1}{8}, \frac{1}{16}, \frac{1}{32}\}$. Therefore the method of estimating the subcarrier spacing (directly related to α) boils down to

the following maximization:

$$\hat{\alpha} = \arg \max_{\tilde{\alpha}} \left\{ \max_{\tilde{\beta} \in \{1/4, 1/8, 1/16, 1/32\}} J_{CC}^{(N_b)}(\tilde{\alpha}, \tilde{\beta}) \right\}. \quad (24)$$

We remind that the state of art methods are based on the maximization of the cost function $J_{CC}^{(0)}(\tilde{\alpha}, \tilde{\beta})$.

In practice, the criterion $J_{CC}^{(N_b)}(\tilde{\alpha}, \tilde{\beta})$ is not available and has to be estimated. We remind that the cyclic correlation $R_y^{(p/\alpha(1+\beta))}(\tilde{\alpha})$ is given by

$$\lim_{M \rightarrow \infty} \frac{1}{M} \sum_{m=0}^{M-1} \mathbb{E}\{y(m + \tilde{\alpha})y^*(m)\} e^{-2i\pi mp/\tilde{\alpha}(1+\tilde{\beta})} \quad (25)$$

and its empirical estimate, denoted by $\hat{R}_y^{(p/\tilde{\alpha}(1+\tilde{\beta}))}(\tilde{\alpha})$, is obtained as follows:

$$\frac{1}{M} \sum_{m=0}^{M-1} y(m + \tilde{\alpha})y^*(m) e^{-2i\pi mp/\tilde{\alpha}(1+\tilde{\beta})}, \quad (26)$$

where M is the number of received samples.

Consequently, $J_{CC}^{(N_b)}(\tilde{\alpha}, \tilde{\beta})$ has to be replaced with $\hat{J}_{CC}^{(N_b)}(\tilde{\alpha}, \tilde{\beta})$ as follows:

$$\hat{J}_{CC}^{(N_b)}(\tilde{\alpha}, \tilde{\beta}) = \frac{1}{2N_b + 1} \sum_{p=-N_b}^{N_b} |\hat{R}_y^{(p/\tilde{\alpha}(1+\tilde{\beta}))}(\tilde{\alpha})|^2.$$

Finally, by replacing the empirical cyclic correlation with Eq. (26), and α, β with their expression in terms of OFDM parameter, we obtain

$$N\hat{T}_c = \arg \max_{\tilde{N}\hat{T}_c} \left\{ \max_{\tilde{D}\hat{T}_c \in \{1/4, 1/8, 1/16, 1/32\}} \hat{J}_{CC}^{(N_b)}(\tilde{N}\hat{T}_c, \tilde{D}\hat{T}_c) \right\}$$

with

$$\hat{J}_{CC}^{(N_b)}(\tilde{N}\hat{T}_c, \tilde{D}\hat{T}_c) = \frac{1}{2N_b + 1} \sum_{p=-N_b}^{N_b} \left| \frac{1}{M} \sum_{m=0}^{M-1} y\left(m + \left\lfloor \frac{\tilde{N}\hat{T}_c}{T_e} \right\rfloor\right) y^*(m) e^{-2i\pi mp/\left\lfloor \frac{\tilde{N}\hat{T}_c}{T_e} \right\rfloor(1+\tilde{D}\hat{T}_c/\tilde{N}\hat{T}_c)} \right|^2.$$

It is clear that, N_b , the number of cyclic frequencies taken into account to perform the estimation has a direct impact on the algorithm performance. Therefore, in the sequel, we provide some insights about the choice of this parameter.

4.2. Influence of design parameter N_b

In this subsection, we discuss the impact of the before mentioned factor by relying on some theoretical derivations.

To evaluate the influence of N_b , we focus on

- mean and variance of the estimated cost function at the true point (α, β) (see Section 4.2.1).
- mean and variance of the estimated cost function at the other points $(\tilde{\alpha}, \tilde{\beta})$ with $\tilde{\alpha} \neq \alpha$ (see Section 4.2.2).

Hereafter, we assume that M is large enough in order to satisfy an asymptotic regime.

4.2.1. Influence of N_b on the estimated cost function at the true point

Due to [17], it is known that $\sqrt{M}(\hat{R}_y^{(p/\alpha(1+\beta))}(\alpha) - R_y^{(p/\alpha(1+\beta))}(\alpha))$ converges, in distribution, to a normal distribution with zero mean and a certain finite variance when M tends to infinity. Thanks to [18], we can deduce that $\sqrt{M}(\hat{J}_{CC}^{(N_b)}(\alpha, \beta) - J_{CC}^{(N_b)}(\alpha, \beta))$ is also asymptotically normal with zero-mean and a finite variance, denoted by σ_1^2 . In order to inspect the impact of N_b on the performance, we have to analyze the variation of $J_{CC}^{(N_b)}(\alpha, \beta)$ and σ_1^2 vs. N_b as done in next proposition.

Proposition 1. *We assume that $\alpha + \beta$ is an integer. We have*

$$J_{CC}^{(N_b)}(\alpha, \beta) = \frac{1}{2N_b + 1} \left| \frac{1}{\alpha(1 + \beta)} \right|^2 \sum_{p=-N_b}^{N_b} \left| \frac{\sin\left(\pi \frac{\beta p}{1 + \beta}\right)}{\sin\left(\pi \frac{p}{\alpha(1 + \beta)}\right)} \right|^2,$$

and

$$\sigma_1^2 = \mathcal{O}(1) + \mathcal{O}\left(\frac{(1 + \sigma^2)^4}{2N_b + 1}\right).$$

Proof of Proposition 1 is drawn in Appendix C. The case where $\alpha + \beta$ is not an integer is not dealt in this paper. Nevertheless, if the condition is not met, the dependance of $J_{CC}^{(N_b)}(\alpha, \beta)$ in term of N_b will not be significantly changed.

One can remark that, when $p > 1/\beta$, the value of $\sin(\pi\beta p/(1 + \beta))/\sin(\pi p/\alpha(1 + \beta))$ is small compared to the value taken around $p = 0$, and the cyclic correlation at lag $p > 1/\beta$ does not provide significant information. Therefore we can reasonably assume that $N_b < 1/\beta$. Then one can see that $J_{CC}^{(N_b)}(\alpha, \beta)$ is a decreasing function of N_b . The greater $J_{CC}^{(N_b)}(\alpha, \beta)$ is, the better the performance should be. On the contrary, the variance increases when N_b decreases. Consequently, based on the mean, we advocate to choose N_b as small as possible; based on the variance, we advocate to choose N_b as large as possible. A trade-off seems to be done to choose relevantly the value of N_b .

4.2.2. Influence of N_b on the estimated cost function at the other points

Once again, we would like to analyze the influence of N_b on the mean and variance of $\hat{J}_{CC}^{(N_b)}(\tilde{\alpha}, \tilde{\beta})$ when $\tilde{\alpha} \neq \alpha$. The result is given in next proposition.

Proposition 2. *The mean of $\hat{J}_{CC}^{(N_b)}(\tilde{\alpha}, \tilde{\beta})$ has the following asymptotic property:*

$$\lim_{M \rightarrow \infty} M \mathbb{E} \hat{J}_{CC}^{(N_b)}(\tilde{\alpha}, \tilde{\beta}) = (1 + \sigma^2)^2 + \mathcal{O}(1).$$

The variation of $\hat{J}_{CC}^{(N_b)}(\tilde{\alpha}, \tilde{\beta})$ around its mean can be analyzed using the following variance defined as

$$\sigma_2^2(\tilde{\alpha}, \tilde{\beta}) = \lim_{M \rightarrow \infty} M^2 \mathbb{E} \left[\hat{J}_{CC}^{(N_b)}(\tilde{\alpha}, \tilde{\beta}) - \mathbb{E} \hat{J}_{CC}^{(N_b)}(\tilde{\alpha}, \tilde{\beta}) \right]^2,$$

which has the following finite value:

$$\sigma_2^2(\tilde{\alpha}, \tilde{\beta}) = \mathcal{O}\left(\frac{(1 + \sigma^2)^4}{2N_b + 1}\right) + \mathcal{O}(1)$$

as long as $\tilde{\alpha} \neq \alpha$.

Proof of Proposition 2 is given in Appendix D.

This proposition says, on one hand, that, as long as $1 \ll \sigma^2$, the asymptotic mean of $\hat{J}_{CC}^{(N_b)}(\tilde{\alpha}, \tilde{\beta})$ does not depend on N_b , and, on the other hand, that the variation of $\hat{J}_{CC}^{(N_b)}(\tilde{\alpha}, \tilde{\beta})$ around its mean is decreasing when N_b increases, for low SNR.

We thus confirm that a trade-off has to be done to choose relevantly the value of N_b .

5. Simulations

In this section we propose to evaluate the proposed techniques by means of numerical simulations.

We have generated an IEEE 802.16.e signal with the following settings: the number of carriers $N = 128$, the useful time duration $NT_c = 102 \mu\text{s}$, and the oversampling ratio $T_c/T_e = 2$. We consider that 20 OFDM symbols are available at the receiver. The transmit signal passes through a multipath fading channel ($L = 10$ paths) where each path delay is uniformly distributed between $[0, \tau_{\max}]$ and each path magnitude is uniformly distributed between $[10^{-2}, 1]$. Except otherwise stated, τ_{\max} is chosen to be equal to $\frac{3}{4}DT_c$ and the ratio $D/N = \frac{1}{32}$. A Gaussian noise has also been added and its variance is defined as

$$\sigma^2 = \frac{T_c}{T_e M} \sum_{m=0}^{M-1} \left| \sum_{l=1}^L \lambda_l s_a(mT_e - \tau_l) \right|^2 10^{-\text{SNR}/10},$$

where M is the number of samples. Except otherwise stated, the number of cyclic frequencies taken into account for the cyclic correlation based method is $N_b = 10$. We have remarked that the GML always outperforms the DML. Therefore, in the sequel, we only plot the GML estimator performance.

The cost functions maximization/minimization have been done with an exhaustive test over the interval $[0.5, 2]NT_c$ for the variable $\hat{N}T_c$ with a step equal to $NT_c/100$ (150 points have hence been tested). The variable $\hat{D}T_c$ belongs to the set of values $\hat{N}T_c \{ \frac{1}{4}, \frac{1}{8}, \frac{1}{16}, \frac{1}{32} \}$. The performance evaluation has been done thanks to Monte-Carlo simulations with 1000 trials for every point.

As we treat an estimation problem, the performance measure may be the mean square error on $\hat{N}T_c$. Nevertheless, our practical problem related to cognitive radio is to identify the right system (WiMAX, WiFi, DAB, DVB-T or 3GPP/LTE, etc) by comparing the $\hat{N}T_c$ to its theoretical value for each considered system. As seen in introduction, the smallest gap between two inter-carrier spacing values is little larger than 1%. Therefore, for our practical system identification issue, we only need an estimation of $1/NT_c$ up to 1%. Consequently rather than considering MSE as performance measure, the performance has been evaluated as the number of correct detection, i.e., the number of realizations for which the $\hat{N}T_c$ is equal to NT_c up to 1%. As a consequence, the probability of wrong detection which includes the probability to take a system for another one, equals 1 minus the probability of correct detection.

Note that a joint estimation of NT_c and DT_c has been performed to estimate the OFDM parameters of interest but the plotted curves only focus on the correct detection

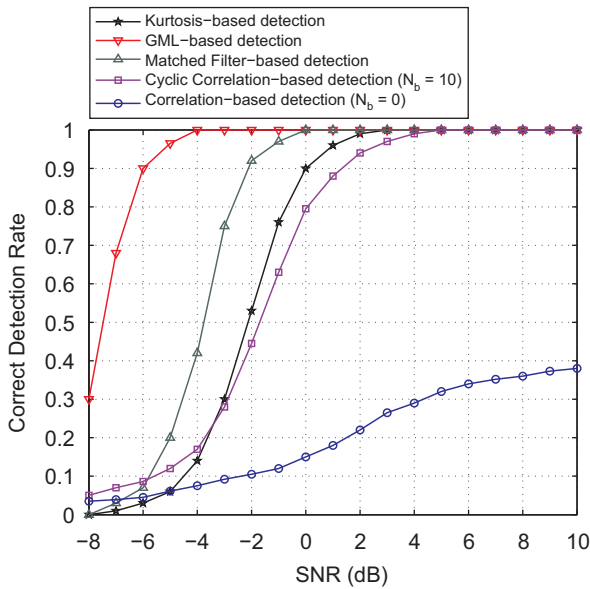


Fig. 1. Correct detection rate vs. SNR ($D/N = \frac{1}{32}$).

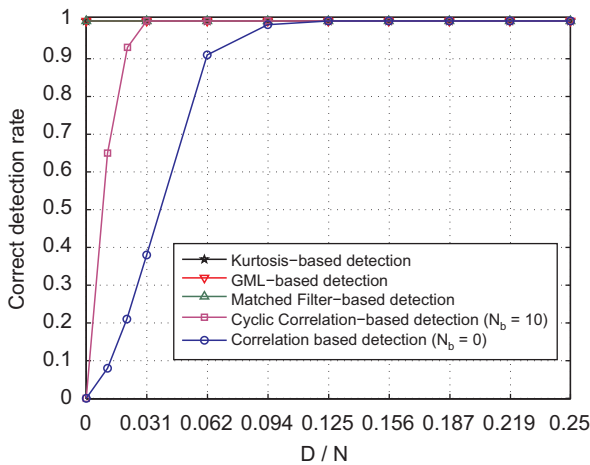


Fig. 2. Correct detection rate vs. the ratio D/N (SNR = 10 dB).

rate of the inter-carrier spacing parameter. Actually we have observed that detections on NT_c or DT_c always yield similar performance.

Firstly, we consider a perfect time and frequency synchronization context. In Fig. 1, we plot the performance of the proposed algorithms and of the state of art method (denoted correlation-based technique) vs. SNR. One can show that all the proposed techniques outperform the standard correlation based method.

In Fig. 2, we display the correct detection rate of the proposed algorithms and of the correlation based method vs. D/N . In order to inspect properly only the impact of the ratio between the cyclic prefix and the useful part durations on the performance, simulations are done here with AWGN channel. As stated in the Introduction, the state of art technique falls down when the length of the

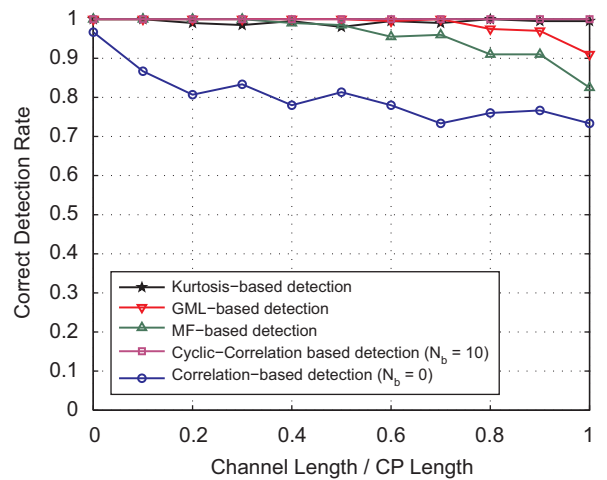


Fig. 3. Correct detection rate vs. the channel length ($D/N = \frac{1}{8}$, SNR = 10 dB).

cyclic prefix is small compared to the length of the useful part of the OFDM signal which may occur for DVB-T and WiMax signals (D/N belongs to $\{\frac{1}{32}, \frac{1}{16}, \frac{1}{8}, \frac{1}{4}\}$). The cyclic correlation based approach still performs well except for $D/N = 0$ (no correlation within the received signal). We show also that the other proposed approaches (GML, matched filter and kurtosis minimization) achieve good performance whatever the ratio D/N and we can conclude that these approaches are independent of the encountered cyclic prefix length. Consequently, all the proposed algorithms are perfectly adapted to recognize OFDM systems in both cognitive radio and military contexts and seem to be particularly attractive.

In Fig. 3, we plot the performance of the proposed techniques and of the correlation based method vs. the channel impulse response length. While the standard correlation based technique is the most affected by the frequency selective channel, the use of other cyclic frequencies which leads to the proposed cyclic correlation based method enables to improve the detection efficiency significantly. Thus the novel second order based technique is more robust. The other proposed techniques are robust to frequency-selective channel, even the GML and the matched filter techniques albeit initially derived under AWGN channel assumption.

In Fig. 4, the algorithms performance have been plotted in function of the number of available symbols. As expected, the correlation methods require much symbols to perform the recognition since they are based on the OFDM symbols statistical properties, whereas the other methods rely on the transmitted data symbols statistics.

We now consider that time and/or frequency offset occur. For the methods proposed in Section 3, an additional loop has been added to perform a joint estimation of the offset and the parameters of interest. As for the parameters \hat{NT}_c and \hat{DT}_c , and exhaustive search is performed. The time offset has been randomly chosen in the set $[0, NT_c + DT_c]$ with a uniform law. The tested offset takes values in the set $[0, \hat{NT}_c + \hat{DT}_c]$ with a step

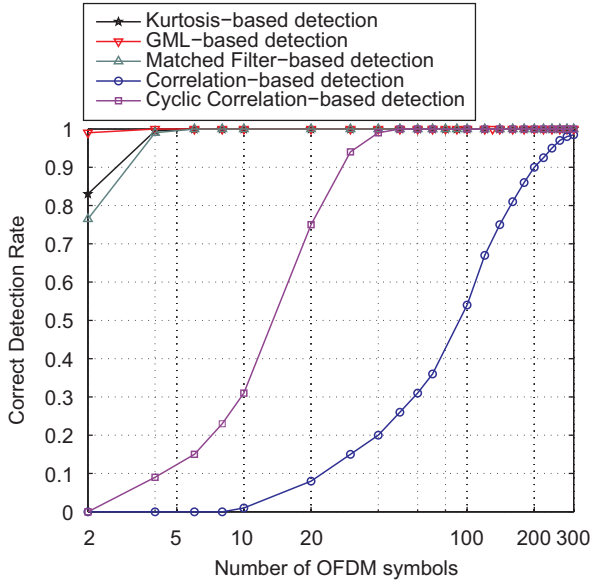


Fig. 4. Correct detection rate vs. number of available symbols ($D/N = \frac{1}{32}$, SNR = 0 dB).

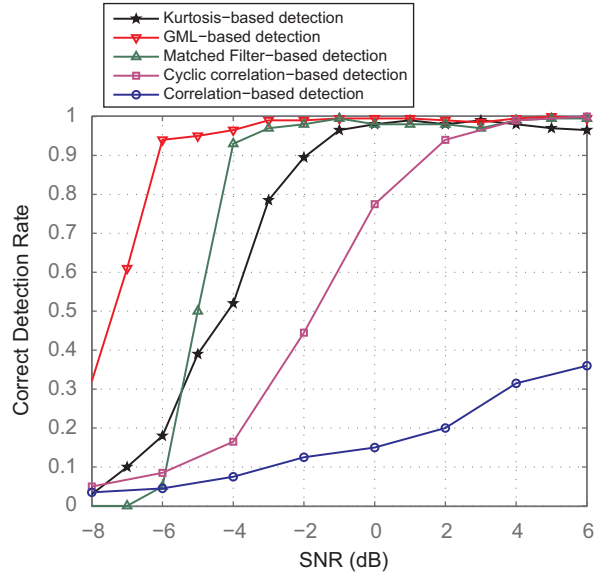


Fig. 6. Correct detection rate vs. SNR including a time offset estimation ($D/N = \frac{1}{32}$).

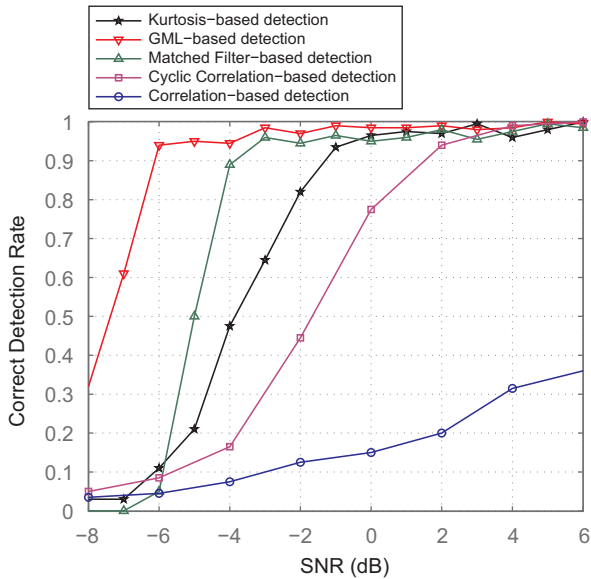


Fig. 5. Correct detection rate vs. SNR including a frequency offset estimation ($D/N = \frac{1}{32}$).

equal to $(\hat{N}T_c + \hat{D}T_c)/10$. The frequency offset is randomly chosen with an uniform law in $[0, 1/NT_c]$. The tested value belongs to $[0, 1/\hat{N}T_c]$ with a step of $1/10\hat{N}T_c$.

The results are shown in Fig. 5 for the frequency offset missynchronization and in Fig. 6 for the time-offset missynchronization. As expected, the second order based approaches are not disturbed by frequency and time missynchronization. In contrast, the methods developed in Section 3 (kurtosis minimization, GML and matched filter) offer slightly degraded performance although offsets estimation step have been carried out.

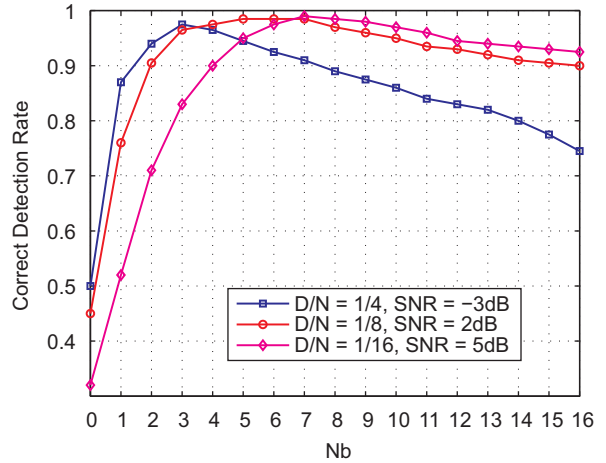


Fig. 7. Correct detection rate of cyclic correlation based algorithm vs. the number of cyclic frequencies N_b .

Based on these illustrations, the GML seems to be the method which outperforms the others. Nevertheless, the reader will easily understand that if the computational time were taken into account, the methods presented in Section 3 are penalized in regard to the method proposed in Section 4.

In Fig. 7, the performance of the cyclic correlation based method is studied vs. the number of cyclic frequencies N_b for different cyclic prefix (CP) lengths. As the performance of this method depends on the length of the cyclic prefix, we have chosen the SNR for each tested CP accordingly. We show that for each CP length, a trade-off has to be done for selecting the value of N_b ensuring the best performance. By comparing the different curves, one can observe that the best value for N_b is lower than N/D .

6. Conclusion

Four new methods for blind identification of the modulation parameters of OFDM based systems have been proposed in this paper. These four algorithms that exploit different principles have been sorted in two categories. The first one contains the algorithms with time and frequency synchronization steps. The three proposed algorithms are based on various techniques: (i) kurtosis minimization, (ii) maximum likelihood, (iii) matched filter. The second kind of algorithms are the one that do not need a synchronization step, including the state of art methods, and the algorithm based on cyclic frequencies estimation.

Most theoretical developments have been done assuming a flat fading channel, but general contexts have been numerically simulated to estimate the robustness of the proposed algorithms. As shown in the section devoted to simulations, there is no algorithm that outperforms the others in every contexts. Nevertheless, in every simulated contexts, all the proposed algorithms have much better performance than the state of art methods.

Appendix A. Proof of Theorem 1

Without loss of generality, we only focus on the first estimated OFDM block. According to Eqs. (2) and (5), the first estimated OFDM block is composed by

$$r_{0,p} = \sum_{l=1}^L \lambda_l s_a(pT_e + \widetilde{DT}_c - \tau_l), \quad \forall p \in \{0, \widetilde{P} - 1\}.$$

Using Eqs. (6) and (1), the decoded symbols $\hat{a}_{0,v}$ writes then, $\forall v \in \{0, N\}$

$$\hat{a}_{0,v} = \frac{1}{\sqrt{PN}} \sum_{l=1}^L \hat{a}_{0,v}^{(l)} \quad (27)$$

with

$$\hat{a}_{0,v}^{(l)} = \sum_{k \in \mathbb{Z}} \sum_{n=0}^{N-1} \tilde{a}_{k,n}^{(l)} \sum_{p=0}^{\widetilde{P}-1} e^{-2i\pi p T_e (n/NT_c - v/\widetilde{NT}_c)} \lambda_l g_a(pT_e + \widetilde{DT}_c - \tau_l - kT_s) \quad (28)$$

and

$$\tilde{a}_{k,n}^{(l)} = a_{k,n} e^{-2i\pi(n/NT_c)(\widetilde{DT}_c - DT_c - \tau_l - kT_s)}. \quad (29)$$

We will first show that, for each path l , we get

$$\kappa(\hat{a}_{0,v}^{(l)}) \geq \kappa(\tilde{a}_{k,n}^{(l)}), \quad \forall k \quad (30)$$

and the equality holds for one particular $k = k_0(l)$ if and only if the conditions of Theorem 1 are satisfied, i.e., if the decoded symbol $\hat{a}_{0,v}^{(l)}$ is proportional to one $\tilde{a}_{k_0(l),v}^{(l)}$. Due to Eq. (29), it is equivalent to be proportional to $\tilde{a}_{k_0(l),v}^{(l)}$ and to the transmit symbol $a_{k_0(l),v}$.

As the summation over p is finite in Eq. (28) and as the function $g_a(t)$ has a finite support, the summation over k in Eq. (28) is also finite. Let Ω_l be the following set:

$$\Omega_l = \{k | \exists p \in \{0, \widetilde{P} - 1\} \text{ s.t. } g_a(pT_e + \widetilde{DT}_c - \tau_l - kT_s) = 1\}.$$

Let us consider that $\text{card}(\Omega_l) > 1$. Under such an assumption, it is clear that the decoded symbol $\hat{a}_{0,v}^{(l)}$ depends at least from 1 transmit symbols of each transmit OFDM symbol which index is in Ω_l . So $\hat{a}_{0,v}^{(l)}$ is a linear combination of several symbols which implies that the inequality of Eq. (30) is a strict inequality. Consequently, in order to obtain equality in Eq. (30), we need $\text{card}(\Omega_l) = 1$. Let us now consider that $\text{card}(\Omega_l) = 1$. Let $k_0(l)$ be the unique element of Ω_l . Under this assumption, we have that $r_{0,p}$ for any $p \in \{0, \widetilde{P} - 1\}$ belongs to the same k_0 th transmit OFDM symbol. Then $\hat{a}_{0,v}^{(l)}$ simplifies as follows:

$$\hat{a}_{0,v}^{(l)} = \lambda_l \sum_{n=0}^{N-1} \tilde{a}_{k_0(l),n}^{(l)} e^{i\theta_n} \frac{\sin\left(\pi \frac{\widetilde{P}T_e}{NT_c} \left(n - v \frac{NT_c}{\widetilde{NT}_c}\right)\right)}{\sin\left(\pi \frac{T_e}{NT_c} \left(n - v \frac{NT_c}{NT_c}\right)\right)},$$

where θ_n still depends on n .

Once again, as $\hat{a}_{0,v}^{(l)}$ is a linear combination of $\tilde{a}_{k_0(l),n}^{(l)}$, Eq. (30) holds. Equality occurs when the weights of the linear combination vanish except one. These weights are zero if and only if it exists n_0 such that

$$\begin{cases} \frac{\sin\left(\pi \frac{\widetilde{P}T_e}{NT_c} \left(n - v \frac{NT_c}{\widetilde{NT}_c}\right)\right)}{\sin\left(\pi \frac{T_e}{NT_c} \left(n - v \frac{NT_c}{NT_c}\right)\right)} \neq 0 & \text{if } n = n_0, \\ \frac{\sin\left(\pi \frac{\widetilde{P}T_e}{NT_c} \left(n - v \frac{NT_c}{\widetilde{NT}_c}\right)\right)}{\sin\left(\pi \frac{T_e}{NT_c} \left(n - v \frac{NT_c}{NT_c}\right)\right)} = 0 & \text{otherwise.} \end{cases}$$

As $\widetilde{P} = \lfloor \widetilde{NT}_c / T_e \rfloor$, we have that $\widetilde{P}T_e / NT_c$ is close to \widetilde{NT}_c / NT_c if N is large enough. One can see that the last property is satisfied if and only if $\widetilde{NT}_c = NT_c$ and $n_0 = v$, i.e., if $\hat{a}_{0,v}^{(l)}$ is proportional to $\tilde{a}_{k_0(l),v}^{(l)}$ and so to $a_{k_0(l),v}$.

Thanks to (27), it is then straightforward to conclude to the kurtosis of $\hat{a}_{0,v}$ is minimal if and only if $\forall l, k_0(l) = k_0$. Note that this condition can be achieved as long as $\tau_l < DT_c$. $\hat{a}_{0,v}$ is then proportional to $a_{k_0,v}$.

This concludes the first part of Theorem 1 (associated with the first inequality provided in Theorem 1).

The second part of Theorem 1 (associated with the second inequality provided in Theorem 1) is proven as follows: for each decoded symbol $\hat{a}_{k,v}$, the first part of Theorem 1 says that the kurtosis reaches its global minimum value if and only if $\widetilde{NT}_c = NT_c$ and $r_{k,p}$ for $p \in \{0, \widetilde{P} - 1\}$ belong to the same transmit OFDM symbol. The kurtosis of the estimated sequence of symbols reaches hence its global minima if both conditions are satisfied for all values of k and n .

Equality $\widetilde{NT}_c = NT_c$ is thus trivial given the first part of Theorem 1. Equality $\widetilde{DT}_c = DT_c$ is deduced from the second condition provided in the first part of the theorem. Indeed, if $\widetilde{DT}_c \neq DT_c$, one can always find a k_* such that the set of points $r_{k_*,p}$ for $p \in \{0, \widetilde{P} - 1\}$ belongs to two OFDM symbols. Then,

$\kappa(\hat{a}_{k,v}) > \kappa(a)$ and equality between the two kurtosis leads to $\widetilde{DT}_c = DT_c$ which concludes the proof.

Appendix B. Proof of Theorem 2

In noiseless flat-fading channel with perfect synchronization, we have $\mathbf{y} = \mathbf{F}_\theta \mathbf{a}$ with i.i.d. data vector \mathbf{a} . Then this leads to

$$J_{\text{MF}}(\tilde{\theta}) = \frac{\text{Tr}(\mathbf{F}_\theta^{\text{H}} \mathbf{F}_\theta \mathbf{F}_\theta^{\text{H}} \mathbf{F}_\theta)}{\|\mathbf{F}_\theta \mathbf{F}_\theta^{\text{H}}\|_F}.$$

Let $\mathbf{A} = \mathbf{F}_\theta$ and $\mathbf{B} = \mathbf{F}_\theta$. Due to the new notation, we have

$$J_{\text{MF}}(\tilde{\theta}) = \frac{\text{Tr}(\mathbf{A}^{\text{H}} \mathbf{B} \mathbf{B}^{\text{H}} \mathbf{A})}{\|\mathbf{A} \mathbf{A}^{\text{H}}\|_F} = \frac{\|\mathbf{A}^{\text{H}} \mathbf{B}\|_F^2}{\|\mathbf{A} \mathbf{A}^{\text{H}}\|_F}.$$

First of all, we would like to prove that the following inequality is satisfied:

$$\frac{\|\mathbf{A}^{\text{H}} \mathbf{B}\|_F^2}{\|\mathbf{A} \mathbf{A}^{\text{H}}\|_F} \leq \|\mathbf{B} \mathbf{B}^{\text{H}}\|_F$$

and that the equality holds if and only if $\mathbf{A} \mathbf{A}^{\text{H}}$ is proportional to $\mathbf{B} \mathbf{B}^{\text{H}}$, i.e., if and only if $\mathbf{F}_\theta \mathbf{F}_\theta^{\text{H}}$ is proportional to $\mathbf{F}_\theta \mathbf{F}_\theta^{\text{H}}$.

Let A_{ij} and B_{ij} be the element of the i th row and j th column of \mathbf{A} and \mathbf{B} , respectively.

$$\|\mathbf{A}^{\text{H}} \mathbf{B}\|_F^2 = \sum_{i=1}^{\widetilde{KN}} \sum_{j=1}^{\widetilde{KN}} \left| \sum_{l=1}^M (A^{\text{H}})_{il} B_{lj} \right|^2 \quad (31)$$

$$= \sum_{l=1}^M \sum_{l'=1}^M \left(\sum_{i=1}^{\widetilde{KN}} A_{il}^* A_{li} \right) \left(\sum_{j=1}^{\widetilde{KN}} B_{lj} B_{l'j}^* \right). \quad (32)$$

For the sake of simplicity, we introduce the following notations: let $\mathbf{V} = \mathbf{A} \mathbf{A}^{\text{H}}$ and $\mathbf{W} = \mathbf{B} \mathbf{B}^{\text{H}}$ be the matrices for which the elements are expressed as

$$V_{ll'} = \sum_{i=1}^{\widetilde{KN}} A_{il} A_{li}^*, \quad W_{ll'} = \sum_{j=1}^{\widetilde{KN}} B_{lj} B_{l'j}^*$$

for all $l = 1, \dots, M$ and $l' = 1, \dots, M$.

By replacing these expressions into Eq. (32), we get

$$\|\mathbf{A}^{\text{H}} \mathbf{B}\|_F^2 = \sum_{l=1}^M \sum_{l'=1}^M V_{ll'} W_{ll'}. \quad (33)$$

A first application of the Cauchy–Schwartz inequality to the sum of index l' in Eq. (33) leads to

$$\|\mathbf{A}^{\text{H}} \mathbf{B}\|_F^2 \leq \sum_{l=1}^M \left[\left(\sum_{l'=1}^M |V_{ll'}|^2 \right)^{1/2} \left(\sum_{l'=1}^M |W_{ll'}|^2 \right)^{1/2} \right]. \quad (34)$$

Equality holds if and only if it exists constants $\{c_l\}_{l=1, \dots, M}$ such that $V_{ll'} = c_l W_{ll'}^*$.

We consider the following notations:

- $v_l = \left(\sum_{l'=1}^M |V_{ll'}|^2 \right)^{1/2}$,
- $w_l = \left(\sum_{l'=1}^M |W_{ll'}|^2 \right)^{1/2}$.

A second application of the Cauchy–Schwartz inequality to the sum of index l gives

$$\|\mathbf{A}^{\text{H}} \mathbf{B}\|_F^2 \leq \left(\sum_{l=1}^M |v_l|^2 \right)^{1/2} \left(\sum_{l=1}^M |w_l|^2 \right)^{1/2}. \quad (35)$$

Notice that $\sum_{l=1}^M |v_l|^2 = \text{Tr}(\mathbf{V} \mathbf{V}) = \|\mathbf{A}^{\text{H}} \mathbf{A}\|_F^2$ and $\sum_{l=1}^M |w_l|^2 = \text{Tr}(\mathbf{W} \mathbf{W}) = \|\mathbf{B}^{\text{H}} \mathbf{B}\|_F^2$ which proves the sought inequality. Equality holds in Eq. (35) if and only if it exists a constant c' such that $v_l = c' w_l$ for all $l = 1, \dots, M$.

Finally equality holds jointly in Eqs. (34) and (35) if and only if it exists a constant c such that $V_{ll'} = c W_{ll'}^* = c W_{l'l}$ for all $l, l' = 1, \dots, M$, i.e., $\mathbf{V} = \mathbf{A} \mathbf{A}^{\text{H}}$ is proportional to $\mathbf{W} = \mathbf{B} \mathbf{B}^{\text{H}}$.

Now we would like to prove that $\mathbf{A} \mathbf{A}^{\text{H}}$ is proportional to $\mathbf{B} \mathbf{B}^{\text{H}}$, i.e., $\mathbf{F}_\theta \mathbf{F}_\theta^{\text{H}}$ is proportional to $\mathbf{F}_\theta \mathbf{F}_\theta^{\text{H}}$ only leads to $\tilde{\theta} = \theta$.

Using Eq. (13), one can prove that each element of $\mathbf{F}_\theta \mathbf{F}_\theta^{\text{H}}$ for $l = 1, \dots, M$ and $l' = 1, \dots, M$ can be expressed as follows:

$$[\mathbf{F}_\theta \mathbf{F}_\theta^{\text{H}}]_{l,l'} = \begin{cases} \frac{1}{\widetilde{N}} \frac{\sin\left(\pi \frac{\widetilde{N} T_e}{\widetilde{N} T_c} (l-l')\right)}{\sin\left(\pi \frac{T_e}{\widetilde{N} T_c} (l-l')\right)} e^{i\pi(l-l')T_e \widetilde{N}-1/\widetilde{N} T_c} & \text{if } |l-l'|T_e \leq \widetilde{N} T_c + \widetilde{D} T_c \text{ and } l \neq l', \\ 1 & \text{if } l = l', \\ 0 & \text{if } |l-l'|T_e > \widetilde{N} T_c + \widetilde{D} T_c. \end{cases}$$

Each block in $\mathbf{F}_\theta \mathbf{F}_\theta^{\text{H}}$ (except the last one) has $\lfloor (\widetilde{N} T_c + \widetilde{D} T_c) / T_e \rfloor$ rows and \widetilde{N} columns. Consequently, if $\mathbf{F}_\theta \mathbf{F}_\theta^{\text{H}}$ is proportional to $\mathbf{F}_\theta \mathbf{F}_\theta^{\text{H}}$, each block of both matrices must have the same dimensions. Thus, we get $\widetilde{N} T_c + \widetilde{D} T_c = N T_c + D T_c$ and $\widetilde{N} = N$.

By considering l and l' such as $|l-l'|T_e \leq \widetilde{N} T_c + \widetilde{D} T_c$ and $l \neq l'$ and any integer k , proportionality between both matrices leads to

$$\begin{cases} (l-l')T_e \frac{N-1}{\widetilde{N} T_c} = (l-l')T_e \frac{N-1}{N T_c} + 2k + \phi, \\ \frac{\sin\left(\pi \frac{N T_e}{\widetilde{N} T_c} (l-l')\right)}{\sin\left(\pi \frac{T_e}{\widetilde{N} T_c} (l-l')\right)} = |c| \frac{\sin\left(\pi \frac{N T_e}{N T_c} (l-l')\right)}{\sin\left(\pi \frac{T_e}{N T_c} (l-l')\right)}, \end{cases}$$

where $|c|$ and ϕ are the magnitude and the phase of the constant c , $k \in \mathbb{Z}$. Last equalities imply that $c = 1$, $\widetilde{N} T_c = N T_c$, and $\widetilde{D} T_c = D T_c$. This concludes the proof.

Appendix C. Proof of Proposition 1

We recall that $\alpha + \beta$ is assumed to be an integer. Using Eqs. (21) and (25), the cyclic frequency coefficient $R_y^{(p/\alpha(1+\beta))}(\alpha)$ can be expressed as

$$R_y^{(p/\alpha(1+\beta))}(\alpha) = \frac{1}{\alpha(1+\beta)} \sum_{n=\alpha}^{\alpha(1+\beta)-1} e^{-2i\pi n p / \alpha(1+\beta)}.$$

It is then straightforward to deduce the expected result on the asymptotic mean.

To compute the estimator variance, we introduce the vector

$$\mathbf{R}_y = [R_y^{(-N_b/\alpha(1+\beta))}(\alpha), \dots, R_y^{(0)}(\alpha), \dots, R_y^{(N_b/\alpha(1+\beta))}(\alpha)]^T$$

and $\hat{\mathbf{R}}_y$ its estimate. The cost function $\hat{J}_{CC}^{(N_b)}(\alpha, \beta)$ is then given by

$$\hat{J}_{CC}^{(N_b)}(\alpha, \beta) = \frac{1}{2N_b + 1} \hat{\mathbf{R}}_y^H \hat{\mathbf{R}}_y.$$

Thanks to the law of large number, $\hat{\mathbf{R}}_y$ is asymptotically normal, and as $\|\mathbf{R}_y\|^2$ is strictly positive, we deduce that $\sqrt{M}(\hat{J}_{CC}^{(N_b)} - J_{CC}^{(N_b)})$ converges in distribution to $\mathcal{N}(0, 4\Sigma)$ (see [18] for more details). Σ is given by

$$\Sigma = \left(\frac{1}{2N_b + 1} \right)^2 [\mathbf{R}_y^H \mathbf{R}_y] \begin{bmatrix} \Gamma & \Gamma_c \\ \Gamma_c^* & \Gamma^* \end{bmatrix} \begin{bmatrix} \mathbf{R}_y \\ \mathbf{R}_y^* \end{bmatrix},$$

where \mathbf{R}_y^* is the conjugate of \mathbf{R}_y , and

1. $\Gamma = \lim_{M \rightarrow \infty} M \mathbb{E}\{(\hat{\mathbf{R}}_y - \mathbf{R}_y)(\hat{\mathbf{R}}_y - \mathbf{R}_y)^H\}$.
2. $\Gamma_c = \lim_{M \rightarrow \infty} M \mathbb{E}\{(\hat{\mathbf{R}}_y - \mathbf{R}_y)(\hat{\mathbf{R}}_y - \mathbf{R}_y)^T\}$.

The coefficients of Γ are given by

$$[\Gamma]_{k,l} = \lim_M M \mathbb{E}\{ \hat{R}_y^{(-N_b+k/\alpha(1+\beta))}(\alpha) \hat{R}_y^{(-N_b+l/\alpha(1+\beta))}(\alpha)^* - MR_y^{(-N_b+k/\alpha(1+\beta))}(\alpha) R_y^{(-N_b+l/\alpha(1+\beta))}(\alpha)^* \}$$

We get after some calculations:

$$\begin{aligned} & \mathbb{E}\{ \hat{R}_y^{(-N_b+k/\alpha(1+\beta))}(\alpha) \hat{R}_y^{(-N_b+l/\alpha(1+\beta))}(\alpha)^* \} \\ &= R_y^{(-N_b+k/\alpha(1+\beta))}(\alpha) R_y^{(-N_b+l/\alpha(1+\beta))}(\alpha)^* \\ &+ \frac{1}{M^2} \sum_{u,v} R_y(u+\alpha, v) R_y^*(u, v) e^{-2i\pi/\alpha(1+\beta)(k-l)u}. \end{aligned}$$

Hence

$$[\Gamma]_{k,l} = \lim_M \frac{1}{M} \sum_{u,v} R_y(u+\alpha, v) R_y^*(u, v) e^{-2i\pi/\alpha(1+\beta)(k(u+v)-lu)}$$

$R_y(u, v)$ vanishes when $v \neq 0$ and $v \neq \pm\alpha$: if $v = 0$, $R_y^*(u, 0)$ does not depend on u . Hence

$$\begin{aligned} & \lim_M \frac{1}{M} \sum_u R_y(u+\alpha, 0) R_y^*(u, 0) e^{-2i\pi/\alpha(1+\beta)(k-l)u} \\ &= (1 + \sigma^2)^2 \delta(k-l). \end{aligned}$$

When v is equal to $\pm\alpha$, the expression is more complex. We will write it as

$$\begin{aligned} & \lim_M \frac{1}{M} \sum_u R_y(u+\alpha, \pm\alpha) R_y^*(u, \pm\alpha) e^{-2i\pi/\alpha(1+\beta)((k-l)u - k(\pm\alpha))} \\ &= \mathcal{O}(1^2). \end{aligned}$$

The matrix Γ has then the following form:

$$\Gamma = \begin{bmatrix} (1 + \sigma^2)^2 + \mathcal{O}(1) & \mathcal{O}(1) & \mathcal{O}(1) \\ \mathcal{O}(1) & \ddots & \mathcal{O}(1) \\ \mathcal{O}(1) & \mathcal{O}(1) & (1 + \sigma^2)^2 + \mathcal{O}(1) \end{bmatrix}.$$

Similarly, the coefficients Γ_c are given by

$$[\Gamma_c]_{k,l} = \lim_M M \mathbb{E}\{ \hat{R}_y^{(-N_b+k/\alpha(1+\beta))}(\alpha) \hat{R}_y^{(-N_b+l/\alpha(1+\beta))}(\alpha) - MR_y^{(-N_b+k/\alpha(1+\beta))}(\alpha) R_y^{(-N_b+l/\alpha(1+\beta))}(\alpha) \}$$

After some calculations, we also get

$$[\Gamma_c]_{k,l} = \lim_M \frac{1}{M} \sum_{u_1, u_2} R_y(u_1, u_1 - u_2 + \alpha) R_y^*(u_2, -u_1 + u_2 + \alpha) e^{-2i\pi/\alpha(1+\beta)(ku_1 + lu_2)}$$

$[\Gamma_c]_{k,l}$ does not vanishes only when $u_1 = u_2$ which gives

$$[\Gamma_c]_{k,l} = \lim_M \frac{1}{M} \sum_u R_y(u, +\alpha) R_y^*(u, \alpha) e^{-2i\pi/\alpha(1+\beta)(k+l)u} = \mathcal{O}(1^2).$$

The matrix Γ_c has then the following form $\Gamma_c = [\mathcal{O}(1)]$.

The matrix

$$\begin{bmatrix} \Gamma & \Gamma_c \\ \Gamma_c^* & \Gamma^* \end{bmatrix}$$

simplifies hence to

$$\begin{bmatrix} \Gamma & \Gamma_c \\ \Gamma_c^* & \Gamma^* \end{bmatrix} = \begin{bmatrix} (1 + \sigma^2)^2 + \mathcal{O}(1) & \mathcal{O}(1) & \mathcal{O}(1) \\ \mathcal{O}(1) & \ddots & \mathcal{O}(1) \\ \mathcal{O}(1) & \mathcal{O}(1) & (1 + \sigma^2)^2 + \mathcal{O}(1) \end{bmatrix},$$

which leads to the expected result.

Appendix D. Proof of Proposition 2

$M\mathbb{E}\{\hat{J}_{CC}^{(N_b)}(\tilde{\alpha}, \tilde{\beta})\}$ writes as

$$\frac{1}{2N_b + 1} \sum_{p=-N_b}^{N_b} M \mathbb{E}\{ |\hat{R}_y^{(p/\alpha(1+\beta))}(\tilde{\alpha})|^2 \}$$

In terms of the received signal $y(m)$, $M\mathbb{E}\{ |\hat{R}_y^{(p/\alpha(1+\beta))}(\tilde{\alpha})|^2 \}$ equals

$$\begin{aligned} & \frac{1}{M} \sum_{m_1} \mathbb{E}\{ y(m_1 + \tilde{\alpha}) y^*(m_1) y^*(m_2) \\ &+ \tilde{\alpha} y(m_2) \} e^{-2i\pi k(m_1 - m_2)/\alpha(1+\beta)}. \end{aligned} \quad (36)$$

Writing the fourth order moment in terms of the fourth order cumulant, $\mathbb{E}\{ y(m_1 + \tilde{\alpha}) y^*(m_1) y^*(m_2 + \tilde{\alpha}) y(m_2) \}$ expands to

$$\begin{aligned} & \text{cum}(y(m_1 + \tilde{\alpha}), y^*(m_1), y^*(m_2 + \tilde{\alpha}), y(m_2)) \\ &+ \mathbb{E}\{ y(m_1 + \tilde{\alpha}) y^*(m_1) \} \mathbb{E}\{ y^*(m_2 + \tilde{\alpha}) y(m_2) \} \\ &+ \mathbb{E}\{ y(m_1 + \tilde{\alpha}) y(m_2) \} \mathbb{E}\{ y^*(m_1 + \tilde{\alpha}) y^*(m_1) \} \\ &+ \mathbb{E}\{ y(m_1 + \tilde{\alpha}) y^*(m_2 + \tilde{\alpha}) \} \mathbb{E}\{ y^*(m_1) y(m_2) \}. \end{aligned} \quad (37)$$

As $y(m + \tilde{\alpha})$ and $y(m)$ are independent when $\tilde{\alpha} > 0$ and $\tilde{\alpha} \neq \alpha$, the first term vanishes. The second term vanishes since $\tilde{\alpha} \neq \alpha$. The third term vanishes since $y(m)$ is circular. The fourth order moment rewrites hence, in terms of the autocorrelation function of the received signal:

$$\begin{aligned} & \mathbb{E}\{ y(m_1 + \tilde{\alpha}) y^*(m_1) y^*(m_2 + \tilde{\alpha}) y(m_2) \} \\ &= R_y(m_2 + \tilde{\alpha}, m_1 - m_2) R_y^*(m_2, m_1 - m_2). \end{aligned}$$

We deduce from this result that Eq. (36) does not vanish only if $m_1 = m_2$, $m_1 = m_2 + \alpha$ or $m_1 = m_2 - \alpha$. If $m_1 = m_2$, we obtain the sum simplifies to $(1 + \sigma^2)^2$. For the other cases, we get the term $\mathcal{O}(1)$.

To compute this variance we first write $\mathbb{E}|M_{CC}^{(N_b)}(\tilde{\alpha}, \tilde{\beta})|^2$ in terms of the cyclic coefficients. We then apply the decomposition (37) to the cyclic coefficients (instead of applying it to the signal y). We get

$$\begin{aligned} M^2 \mathbb{E}|\hat{J}_{CC}^{(N_b)}(\tilde{\alpha}, \tilde{\beta}) - \mathbb{E}\hat{J}_{CC}^{(N_b)}(\tilde{\alpha}, \tilde{\beta})|^2 \\ = \frac{M^2}{(2N_b + 1)^2} \sum_{k_1, k_2} |\mathbb{E}\{\hat{R}_y^{(k_1/\tilde{\alpha}(1+\tilde{\beta}))}(\tilde{\alpha})\hat{R}_y^{(k_2/\tilde{\alpha}(1+\tilde{\beta}))}(\tilde{\alpha})\}|^2 \\ + \frac{M^2}{(2N_b + 1)^2} \sum_{k_1, k_2} |\mathbb{E}\{\hat{R}_y^{(k_1/\tilde{\alpha}(1+\tilde{\beta}))}(\tilde{\alpha})(\hat{R}_y^{(k_2/\tilde{\alpha}(1+\tilde{\beta}))}(\tilde{\alpha}))^*\}|^2. \end{aligned}$$

The result only requires to compute both expectations using a similar technique as for the asymptotical mean.

The first one $\mathbb{E}\{\hat{R}_y^{(k_1/\tilde{\alpha}(1+\tilde{\beta}))}(\tilde{\alpha})\hat{R}_y^{(k_2/\tilde{\alpha}(1+\tilde{\beta}))}(\tilde{\alpha})\}$ vanishes except if $\tilde{\alpha} = \alpha/2$. The second one can be computed as the expectation that has been computed for the asymptotic mean.

References

- [1] P. Marchand, J.-L. Lacoume, C.L. Martret, Classification of linear modulations by a combination of different orders cyclic cumulants, in: Workshop on High Order Statistics, 1997, p. 47.
- [2] P. Bianchi, P. Loubaton, F. Sirven, Non data aided estimation of the modulation index of continuous phase modulations, IEEE Transactions on Signal Processing 52 (2004) 2847–2861.
- [3] O.A. Dobre, A. Abdi, Y. BarNess, W. Su, A survey of automatic modulation classification techniques classical: approaches and new developments, IET Communications 1 (2007) 137–156.
- [4] O.A. Dobre, A. Punchedewa, S. Rajan, R. Inkol, On the cyclostationarity of OFDM and single carrier linearly digitally modulated signals in time dispersive channels with applications to modulation recognition, in: IEEE Wireless Communications and Networking Conference, 2008, pp. 1284–1289.
- [5] O.A. Dobre, Q. Zhang, S. Rajan, R. Inkol, Second-order cyclostationarity of cyclically prefixed single carrier linear digital modulations with applications to signal recognition, in: IEEE Global Communications Conference, 2008, pp. 1–5.
- [6] M. Shi, W. Su, Blind OFDM systems parameters estimation for software defined radio, in: IEEE International Symposium on New Frontiers in Dynamic Spectrum Access Networks, 2007, pp. 119–122.
- [7] T. Yucek, H. Arslan, OFDM signal identification and transmission parameter estimation for cognitive radio applications, in: IEEE Global Communications Conference, 2007, pp. 4056–4060.
- [8] H. Ishii, G. Wornell, OFDM blind parameter identification in cognitive radios, in: IEEE International Conference on Personal, Indoor and Mobile Radio Communications, 2005, pp. 700–705.
- [9] P. Liu, B.-B. Li, Z.-Y. Lu, F.-K. Gong, A blind time-parameters estimation scheme for OFDM in multi-path channel, in: International Conference on Wireless Communications, Networking and Mobile Computing, 2005, pp. 242–247.
- [10] W. Akmouche, E. Kerhervé, A. Quinquis, Estimation of OFDM signal parameters: time parameters, in: Asilomar Conference on Computer, Circuits and Systems, 2000, pp. 142–146.
- [11] J. Mitola, Cognitive radio: an integrated agent architecture for software defined radio, Ph.D. Thesis, Royal Institute of Technology, Stockholm, Sweden, 2000.
- [12] A. Dandawaté, G. Giannakis, Statistical tests for presence of cyclostationarity, IEEE Transactions on Signal Processing 42 (1994) 2355–2369.
- [13] O. Shalvi, E. Weinstein, New criteria for blind deconvolution of non-minimum phase systems, IEEE Transactions on Information Theory 36 (1990) 312–321.
- [14] S. Houcke, A. Chevreuil, P. Loubaton, Blind equalization: case of an unknown symbol period, IEEE Transactions on Signal Processing 51 (2003) 781–793.
- [15] G. Vazquez, J. Riba, Non data-aided digital synchronization, Edition on Signal Processing Advances in Communications, 2000.
- [16] C. Mosquera, S. Scalise, R. Lopez-Valcarce, Symbol rate estimation for DVB-S2 broadcasting, in: International Workshop on Signal Processing for Space Communications, 2006.
- [17] P. Ciblat, P. Loubaton, E. Serpedin, G. Giannakis, Asymptotic analysis of blind cyclic correlation based symbol rate estimation, IEEE Transactions on Information Theory 48 (2002) 1922–1934.
- [18] P. Brockwell, R. Davis, Time Series: Theory and Methods, Springer Series in Statistics, Springer, Berlin.